

Peptide-Functionalized Hydrogels Modulate Integrin Expression and Stemness in Adult Human Epidermal Keratinocytes

Duncan Davis-Hall, Vy Nguyen, Tyler J. D'Ovidio, Ethan Tsai, Ganna Bilousova, and Chelsea M. Magin*

The extracellular matrix (ECM) controls keratinocyte proliferation, migration, and differentiation through β -integrin signaling. Wound-healing research requires expanding cells in vitro while maintaining replicative capacity; however, early terminal differentiation under traditional culture conditions limits expansion. Here, a design of experiments approach identifies poly(ethylene glycol)-based hydrogel formulations with mechanical properties (elastic modulus, $E = 20.9 \pm 0.56$ kPa) and bioactive peptide sequences that mimic the epidermal ECM. These hydrogels enable systematic investigation of the influence of cell-binding domains from fibronectin (RGDS), laminin (YIGSR), and collagen IV (HepIII) on keratinocyte stemness and β_1 integrin expression. Quantification of 14-day keratin protein expression shows four hydrogels improve stemness compared to standard techniques. Three hydrogels increase β_1 integrin expression, demonstrating a positive linear relationship between stemness and β_1 integrin expression. Multifactorial statistical analysis predicts an optimal peptide combination ([RGDS] = 0.67 mM, [YIGSR] = 0.13 mM, and [HepIII] = 0.02 mM) for maintaining stemness in vitro. Best-performing hydrogels exhibit no decrease in Ki-67-positive cells compared to standards (15% decrease, day 7 to 14; $p < 0.05$, Tukey Test). These data demonstrate that precisely designed hydrogel biomaterials direct integrin expression and promote proliferation, improving the regenerative capability of cultured keratinocytes for basic science and translational work.

and differentiation of stem cells.^[1] A variety of intrinsic and extrinsic factors including extracellular matrix (ECM) composition, physical forces, and neighboring cells^[2] control the balance between self-renewal and differentiation of epidermal stem cells in both healthy and healing skin.^[3,4] Stem cells in the basal layer of the epidermis are attached through integrins (primarily $\alpha_2\beta_1$, $\alpha_3\beta_1$, and $\alpha_6\beta_4$) to a basement membrane comprised of proteins such as fibronectin, laminins, and collagens.^[5,6] Variation in ECM composition and in turn integrin expression within different regions of the epidermis creates distinct adhesive environments that recruit stem cells and modulate their differentiation to fully mature keratinocytes. Downregulation of integrin expression reduces ECM adhesiveness and initiates upward migration of stem cells through the epidermis to the outermost layer of skin.^[6] The signals these cells encounter along the way program differentiation into mature keratinocytes.^[2] Experimental evidence shows that at each stage of differentiation keratinocytes express specific keratin proteins (keratins 14, 10, 5, and 1).


Keratin 14 (K_{14}) denotes progenitor cells with high stemness while keratin 1 (K_1) indicates terminal differentiation.^[7,8] There is growing interest in investigating the extrinsic signals that regulate epidermal stem cell fate and function to use these

1. Introduction

Human epidermis, the most superficial layer of the skin, is a multilayered epithelium maintained through the proliferation

D. Davis-Hall, V. Nguyen, T. J. D'Ovidio, Dr. C. M. Magin
Division of Pulmonary Sciences and Critical Care Medicine
Department of Medicine and Department of Bioengineering
University of Colorado Denver, Anschutz Medical Campus
12700 E 19th Ave, MS C272, Aurora, CO 80045, USA
E-mail: chelsea.magin@cuanschutz.edu

Dr. E. Tsai
Metropolitan State University of Denver
Chemistry and Biochemistry Department
P.O. Box 173362, Campus Box 52, Denver, CO 80217-3362, USA

 The ORCID identification number(s) for the author(s) of this article can be found under <https://doi.org/10.1002/adbi.201900022>.

Dr. G. Bilousova
University of Colorado Anschutz Medical Campus
School of Medicine
Department of Dermatology and Charles C. Gates Center
for Regenerative Medicine
12800 E. 19th Ave, P18-8125, Aurora, CO 80045, USA

DOI: 10.1002/adbi.201900022

Table 1. Summary of targeted epidermal integrins, their ECM ligands, associated peptide binding sequence and known functions in the skin.

Integrin	ECM ligand	Peptide binding sequence	Function in epidermis
$\alpha_v\beta_3$, $\alpha_5\beta_1$ ^{a)}	Fibronectin	RGDS ^[47–49]	Contributes to epidermal migration in wound healing. ^[4]
$\alpha_3\beta_1$	Laminin	YIGSR ^[5,50]	Required for maturation of basement membrane, epidermal-dermal junction and angiogenesis. ^[4]
$\alpha_2\beta_1$	Collagens	CGGEFYFDLRLKGDGK (HepIII) ^[51,52]	May contribute to epidermal migration in wound healing. ^[4]

^{a)}The $\alpha_5\beta_1$ has been shown to interact with the linear peptide sequence RGDS.^[47] However, this binding event is weak and can be strengthened by the addition of the synergistic sequence PHSRN.^[48,49]

cells to improve our knowledge of skin regeneration and for translational applications such as tissue-engineered wound dressings.^[9–11]

Generation of keratinocyte cultures capable of self-renewal in vitro remains important to the biomedical community. Maintaining keratinocyte stemness and proliferation in culture leads to increased regenerative capacity and improved likelihood for success in medical treatments such as cell therapies for heritable diseases^[12] or living skin wound-dressings for severe burns and chronic skin wounds.^[13] Large populations of regenerative cells are required for these applications but current in vitro techniques fail to replicate the stem-like niche of basal keratinocytes in vivo and transplanted cells often fail to regenerate when implanted.^[13] Although human keratinocytes have been cultured ex vivo for over three decades, these cells quickly lose stemness and terminally differentiate during traditional cell culture on glass or tissue-culture polystyrene.^[14] This limitation may arise from the culture method. Cells are often grown and passaged on tissue-culture polystyrene while experiments involving keratinocytes are carried out on protein-coated glass coverslips. Both substrates have supraphysiologically high moduli of elasticity (≈ 3 GPa) that does not accurately imitate human epidermal tissue (≈ 20 kPa).^[15,16] These conditions have been shown to decrease stemness in keratinocytes cultured in vitro and therefore prevent researchers from expanding and studying these cells in their progenitor stage.^[14]

Integrins expressed in response to a particular cell culture substrate play a critical role in regulating epithelial stem cell maintenance. The Watt group found that epidermal stem cells with compromised β_1 integrin expression exhibited reduced adhesiveness and regenerative potential. Overexpression of β_1 rescued this phenotype and led the group to conclude that β_1 integrins help maintain epidermal cell stemness.^[17] Likewise, Baker et al. found that antibodies blocking laminin-binding to the $\alpha_3\beta_1$ integrin inhibited human epithelial-cell proliferation in vitro. Additionally, they reported that re-activating the β_1 integrin restored epithelial-cell regenerative capacity (a hallmark of stemness), especially with the introduction of exogenous collagen.^[18] It is currently recognized that β_1 integrins prevent early terminal differentiation and thus are necessary for healthy keratinocyte growth. Culture microenvironment is a key regulator of the stemness of these epithelial cells. Therefore, reproducible in vitro systems that maintain stem-like primary human epidermal keratinocyte cultures for both basic and translational research endeavors are needed.

Engineering approaches to address the terminal differentiation of keratinocytes in culture have focused on understanding how the underlying substrate can be altered to maintain β_1

integrin expression. Tjin et al. designed peptide sequences that mimicked cell-binding domains derived from fibronectin, laminin, and collagen IV (Table 1). Keratinocytes grown on tissue culture plates coated with these artificial ECM components showed increased attachment, proliferation, and stemness compared to controls.^[3] Similarly, Salber and colleagues showed that sequences derived from laminin and collagen IV increased keratinocyte attachment to poly(dimethylsiloxane) (silicone) surfaces compared to sequences from fibronectin and a combination of peptides, resulting in stronger adhesion than single sequences alone.^[19]

To complement these studies and identify the optimal microenvironment for maintaining keratinocyte stemness in culture, we hypothesized that poly(ethylene glycol) (PEG)-based hydrogels could be precisely designed to mimic the biophysical and biochemical properties of the native epidermal stem cell niche. To test this hypothesis, we implemented a design of experiments (DOE) approach to systematically vary the concentration of three peptide sequences that mimic epidermal ECM binding motifs (Table 1) and iteratively evaluate the effects of different culture platforms on keratinocyte stemness in vitro.^[20–22] Here, we used immunofluorescent staining for keratin proteins K₁₄ and K₁ to quantify stemness, integrin β_1 expression to investigate signaling, and Ki-67 for proliferation. These characteristics were measured on experimental hydrogel platforms decorated with different peptide combinations and concentrations or protein-coated glass coverslip standards. Quantifying stemness and proliferation allowed us to tailor biochemical conditions to optimize maintenance of keratinocyte populations in vitro. These results reveal that hydrogel-based cell culture platforms show promise for promoting keratinocyte self-renewal so that skin regeneration can be more easily investigated in vitro.

2. Results

2.1. Hydrogel Synthesis and Characterization

Hydrogels were formed via a photoinitiated thiol–ene reaction.^[16] Briefly, PEG-norbornene (PEG-NB; 8-arm, 10 kg mol⁻¹) was reacted with a short dithiol crosslinker (dithiothreitol; DTT) and cysteine-terminated peptide sequences (Figure 1a) in the presence of lithium phenyl (2,4,6-trimethylbenzoyl)phosphinate (LAP) photoinitiator and 365 nm light (10 mW cm⁻², 5 min). Results showed that hydrogels ranging from 5 to 10 wt% PEG-NB exhibited elastic modulus values (*E*) ranging from 5.3 to 39.8 kPa (Figure 1b). Modulus increased with increasing polymer content as expected. Hydrogels consisting

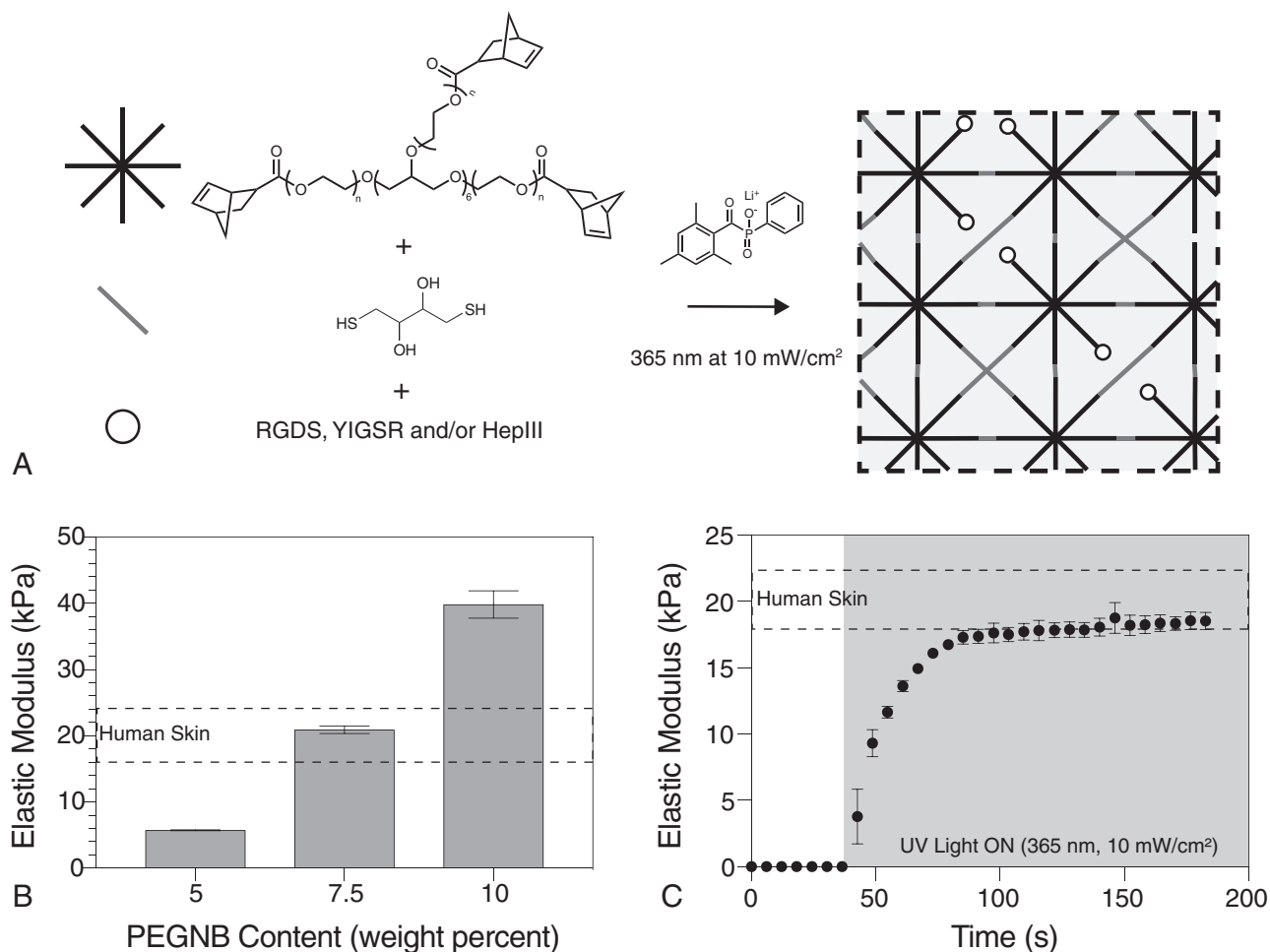


Figure 1. a) Hydrogels were synthesized by combining PEG-norbornene with dithiothreitol (DTT), short cysteine-terminated peptide sequences, and a photoinitiator in the presence of 365 nm light to produce peptide-functionalized cell culture platforms. b) Parallel-plate rheology results confirmed that hydrogel platform mechanical properties could be tuned to match those of human skin ($E \approx 15\text{--}25$ kPa).^[16] Columns report mean \pm SEM, $n = 5$. c) Dynamic rheological characterization during polymerization confirmed that the network was fully formed within 60 s of exposure to 365 nm light. Symbols represent mean \pm SEM, $n = 5$.

of 7.5 wt% PEG-NB best approximated human skin ($E = 20.9 \pm 0.56$ kPa) and were selected as the experimental platform for the following studies. Dynamic rheological measurements were acquired on the 7.5 wt% formulation during polymerization (Figure 1c). The plot of elastic modulus versus time showed that polymerization began immediately after exposure to light (365 nm; 10 mW cm^{-2}) and was complete within 60 s of exposure.

Equilibrium swelling was also measured and compared to theoretical swelling values as a complementary technique for quantifying network formation and defect concentration. Experimental hydrogels reached equilibrium swelling after 6 h of immersion in phosphate-buffered saline (PBS) (Figure S1, Supporting Information). The final average experimental volumetric equilibrium swelling ratio ($Q = 12.1$) was compared to the calculated theoretical swelling ratio ($Q_{\text{theo}} = 10.9$) and was found to fall within the 95% confidence interval defined by experimental results (Supporting Information). Thus, the hydrogel networks presented here were formed with very few defects.

2.2. Evaluation of Stemness

A design of experiments (DOE) approach identified a multifactorial experiment that systematically determined the individual and combinatorial effects of each peptide or protein binding sequence concentration on keratinocyte stemness. Eight experimental platforms with various combinations and concentrations of all three binding motifs represented by peptide mimics in experimental hydrogel platforms were compared to whole proteins deposited onto glass coverslip controls (Table 2). The goal of this screen was to identify the optimal concentration of binding sequences within a hydrogel platform to maximize

Table 2. Hydrogel and standard binding motif concentrations.

Platform	[HepIII] [mM]	[RGDS] [mM]	[YIGSR] [mM]
Hydrogel \uparrow	0.04	0.67	0.13
Hydrogel \downarrow	0.02	0.17	1.5
Standard \uparrow	48	4.5	0.04

keratinocyte stemness compared to standard cell culture techniques. Quantification of immunofluorescent staining (Figure 2a) for K_{14} and K_1 (Figure 2b) showed that four experimental platforms (gray) significantly improved stemness at day 14 in culture compared to the standard (white), where a higher ratio of K_{14} to K_1 indicated an increase in the number of cells with the potential for self-renewal. The most effective hydrogel platforms showed a more than fivefold increase in stemness over the control (mean $K_{14}:K_1$ of 19.1 versus mean $K_{14}:K_1$ of 3.4, $p < 0.05$, Dunnett's Test).

The binding motifs RGDS found in fibronectin and YIGSR found in laminin both improved stemness with increasing concentration while the HepIII binding site from collagen IV decreased stemness with increasing concentration (Figure 2c). Prediction profiles for hydrogel platforms indicated greater potential stemness in hydrogels could be achieved by maximizing concentrations of RGDS (0.67 mM) and YIGSR (0.13 mM) while minimizing HepIII (0.02 mM). Effects analysis of stemness results including both main and interaction effects revealed the influence of binding motifs on stemness as measured by $K_{14}:K_1$ immunofluorescence (Figure 2d). While none of the reported effects magnitudes were statistically significant, the interaction between RGDS and YIGSR concentrations was identified as the factor that exhibited the highest level of influence over keratinocyte stemness on hydrogel platforms.

2.3. Evaluation of β_1 Integrin Expression

To investigate the connection between stemness and integrin-mediated ECM signaling, β_1 integrin expression was measured by immunofluorescence (Figure 3a) on day 2 of culture. This time point was selected based on previous work in the field reporting β_1 integrin expression peaks at 48 h after seeding in on samples.^[18,23] Interestingly, three hydrogel conditions showed statistically higher β_1 integrin expression than the standard (Figure 3b; $p < 0.05$, Dunnett's Test) and all of these platforms showed increased stemness compared to the standard. These measurements resulted in a non-zero ($p = 0.0072$) positive correlation between stemness and integrin expression (Figure 3c). The best-performing platform from both stemness and integrin expression assays contained the highest concentrations of all three peptide binding motifs and was selected for subsequent proliferation and migration assays.

2.4. Adult Human Epidermal Keratinocytes Proliferation and Migration

Immunofluorescent staining for Ki-67 measured adult human epidermal keratinocyte (HEKA) proliferation after 2, 7, and 14 days in culture. Cells were counterstained for DAPI and proliferation was assessed by counting proportion of Ki-67-positive cells in culture (Figure 4a). HEKAs grown on standard protein-coated substrates showed a significant 15% decrease in proliferation from day 7 to 14 ($p < 0.05$, Tukey Test), while cells grown on hydrogels showed no difference in proliferation over 14 days (Figure 4b). HEKA migration was assessed with a modified scratch-wound assay and no significant differences were detected

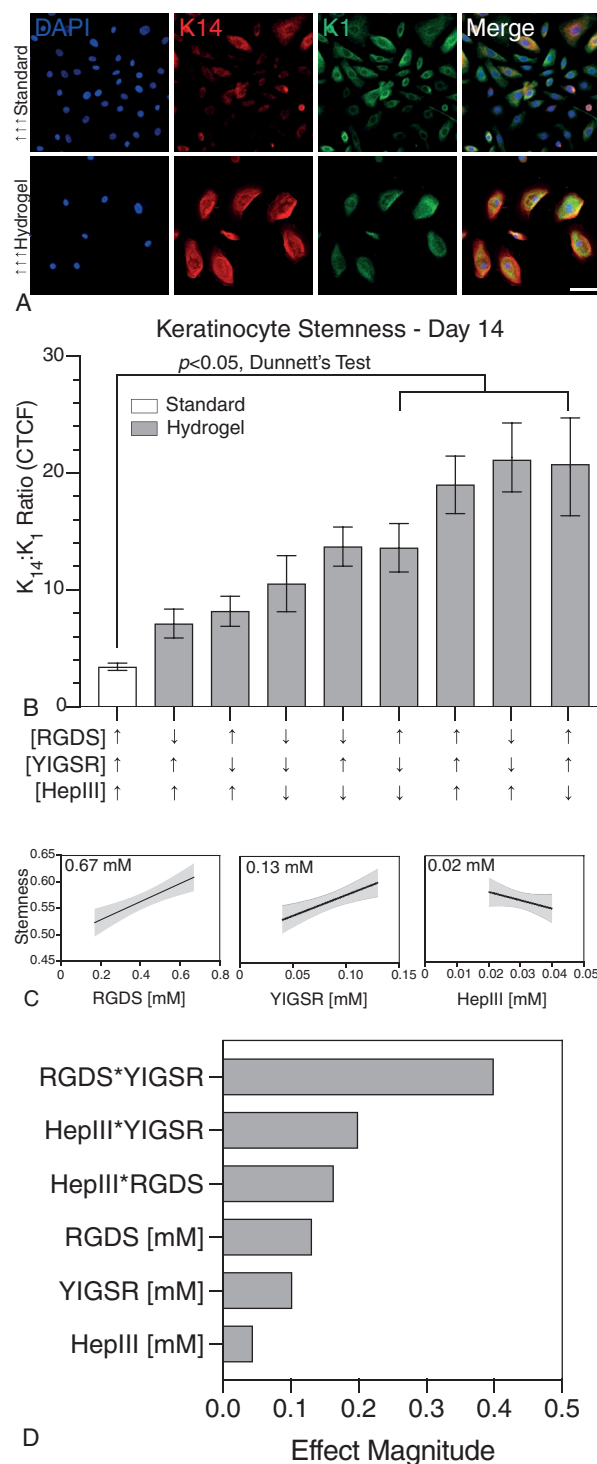


Figure 2. a) Representative fluorescent images of K_{14} (red) and K_1 (green) immunostaining on the standard and one of the best-performing hydrogel surfaces. Scale bar, 50 μm . b) Keratinocyte stemness on hydrogel (gray) and standard (white) platforms representing a multifactorial screen measured by calculating the ratio of K_{14} to K_1 corrected total cell fluorescence. Columns represent mean \pm SEM, $n = 3$. c) Prediction profiles of stemness versus binding motif concentrations showed trends that can maximize stemness. Shaded region represents 95% confidence interval of multifactorial analysis. d) Main and interaction effects of binding motif concentrations in hydrogel platforms. Bars represent parameter estimates.

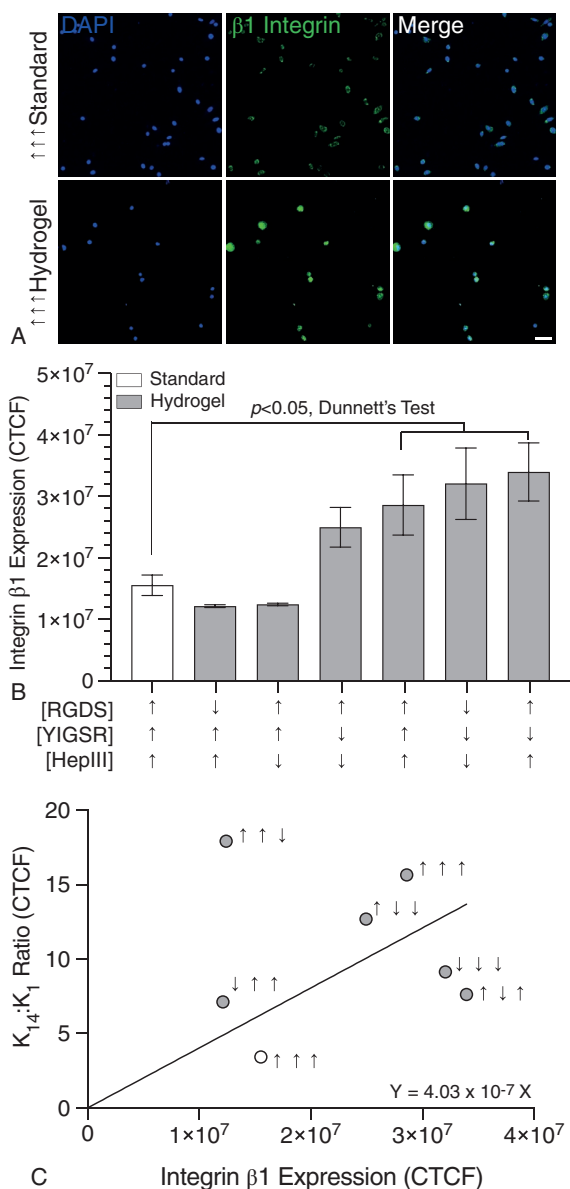


Figure 3. a) Representative fluorescent images of the standard and one of the best-performing hydrogel surfaces for β_1 integrin expression (green) show increased levels of β_1 expression on hydrogels versus the standard. Scale bar, 50 μm . b) β_1 integrin expression as measured by corrected total cell fluorescence at day 2 on hydrogel platforms (dark gray) and standards (light gray). Columns represent mean \pm SEM, $n = 4$. c) Keratinocyte stemness ($K_{14}:K_1$) plotted versus β_1 integrin expression. Dark gray dots represent hydrogel platform mean values and white dots represent standard platform mean values. Fit line is the result of a linear regression and indicates a positive correlation.

in migration between cells grown on standard and hydrogel platforms at day 14 (Figure S2, Supporting Information).

3. Discussion

Previous research has shown peptide sequences that mimic ECM binding domains can improve epidermal cell adhesion

and function in vitro. Specifically, incorporating binding sequences derived from fibronectin, laminin, and collagen IV into culture substrates has increased attachment, proliferation, and stemness of keratinocytes.^[3] Moreover, surfaces that include a combination of peptide-binding sequences from multiple ECM proteins can improve keratinocyte adhesion to a greater degree than a single binding motif.^[19] We have built on that base of knowledge by analyzing the optimal concentration of binding motifs on hydrogel substrates with mechanical properties that match human skin to improve keratinocyte culture outcomes including stemness, integrin expression, and proliferation.

This report highlights a systematic method for using hydrogel biomaterials to improve epithelial cell culture conditions. A DOE approach in combination with a versatile PEG-based thiol-ene hydrogel platform identified combinations and concentrations of ECM binding sequences that enhanced maintenance of keratinocyte stemness and proliferation in vitro. Specific binding motifs tethered to hydrogels with an elastic modulus representative of epidermal tissue elicited changes in β_1 integrin expression, increased stemness measured by K_{14} and K_1 (a progenitor marker and terminal differentiation marker, respectively),^[7] and extended HEKA proliferative lifespan.

Bio-inspired cell culture platforms based on peptide-functionalized PEG hydrogels increased HEKA stemness compared to stiff protein-coated standard substrates. Significant improvements in self-renewal properties were measured by $K_{14}:K_1$ immunofluorescence in four hydrogel platforms ($\uparrow\uparrow\downarrow$, $\downarrow\downarrow\uparrow$, $\uparrow\uparrow\uparrow$, and $\uparrow\downarrow\downarrow$) when compared to protein-coated glass coverslip standards ($p < 0.05$, Dunnett's Test). DOE analysis showed that the interaction between RGDS and YIGSR binding regions were the major contributors to HEKA stemness with HepIII contributing the least. These results agreed with long-standing work in the field of skin wound-healing research. Epidermal cells have been shown to readily adhere to fibronectin-binding motifs, but not in the presence of collagen-binding regions.^[24] Previous research has shown that laminin and collagen IV encouraged epidermal cell binding when combined with low concentrations of fibronectin.^[25] Results presented here followed that trend, with YIGSR making up an important component for both hydrogels and standard platforms.

An increase in β_1 integrin expression was also measured in cells cultured on hydrogel platforms compared to standard platforms. HEKAs grown on three hydrogels ($\uparrow\downarrow\downarrow$, $\downarrow\downarrow\downarrow$, and $\uparrow\uparrow\uparrow$) exhibited significantly greater β_1 integrin expression than the standard platform ($p < 0.05$, Dunnett's Test). Upregulation of this integrin may have played a key role in improved stemness measured in HEKAs cultured on peptide-functionalized hydrogels. The integrin β_1 has been linked to basal keratinocyte progenitor populations—this protein was upregulated in conjunction with p63, a commonly-accepted stem cell marker.^[26] In addition, foundational research has established that cells with greater expression of β_1 protein adhered to ECM proteins and self-renewed more readily than other cell populations.^[27] Keratinocytes undergoing terminal differentiation showed progressive decreases in integrin expression.^[28,29] The increased β_1 expression and stemness measured on hydrogel platforms provided evidence that these biomaterials may more closely

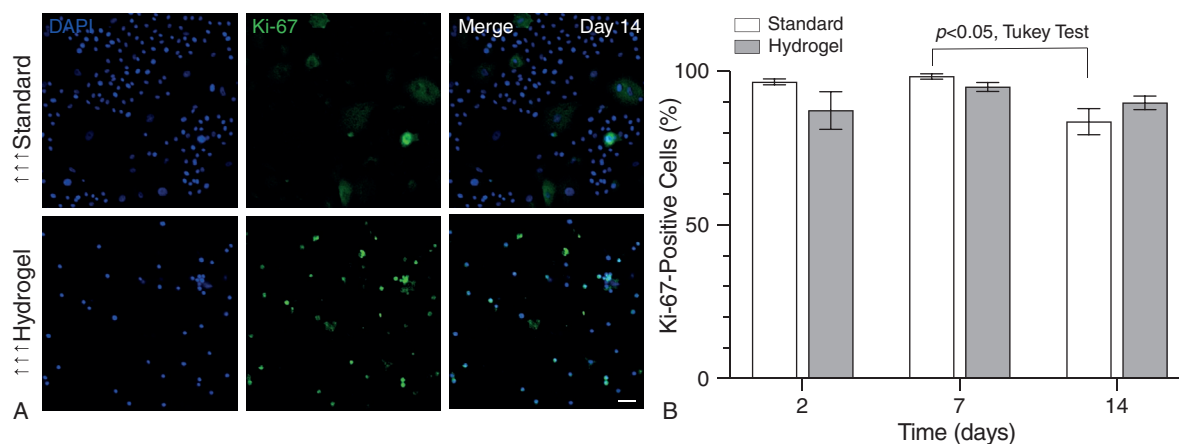


Figure 4. a) Representative fluorescent microscopy images comparing proliferation (Ki-67, green) between one of the best-performing hydrogels and the standard platform on day 14. Scale bar, 1 mm. b) Quantification of Ki-67-positive cells demonstrates no significant difference in proliferation on the hydrogel over 14 days, while a significant decrease was observed on the standard between days 7 and 14 ($p < 0.05$, Tukey Test). Columns represent mean \pm SEM, $n = 4$.

replicate the basal stem cell niche present in native human skin than protein-coated glass.

Hydrogel platforms also maintained greater numbers of proliferating cells as measured by Ki-67 immunofluorescence, a nuclear protein not expressed in the G0 stage of the cell cycle but present in increasing concentrations as the cell progresses through the cell cycle and peaking during mitosis, than standard culture platforms. HEKAs grown on the $\uparrow\uparrow\uparrow$ hydrogel platform did not show a change in proliferation during 14 days of culture while cells grown on the corresponding standard platform demonstrated a 15% decrease in Ki-67-positive cells between day 7 and day 14 ($p < 0.05$, Tukey Test). These results suggest that keratinocytes grown on hydrogel substrates with a modulus matching physiologic values had a longer proliferative lifespan than those grown using standard culture conditions. Work by Salber et al. and Tjin et al. established the benefits of culturing keratinocytes on surfaces modified with peptide-binding motifs. However, these studies focused on poly(dimethylsiloxane) and glass coverslips, which both have significantly higher modulus values than native human epidermis.^[3,19] The peptide-functionalized hydrogel platforms developed here not only matched epidermal modulus measurements reported in the literature, but also optimized the concentration of three important ECM binding regions to maximize proliferation and further improve keratinocyte stemness.

4. Conclusion

Collectively, these results demonstrate the potential for biomaterial-based cell culture methods to improve in vitro keratinocyte culture. A synthetic PEG-based hydrogel was precisely designed and optimized to achieve the biophysical and biochemical properties that produced keratinocytes with fivefold greater $K_{14}:K_1$ ratio, twofold greater β_1 integrin expression, and no loss in Ki-67 proliferation compared to keratinocytes grown on protein-coated glass. This evidence supports the hypothesis

that bio-inspired engineered cell culture techniques can offer improved cell outcomes compared to traditional culture methods. Research investigating the re-epithelialization stage of the wound-healing process relies on maintaining cultures of stem-like keratinocytes in vitro. Synthetic polymeric materials, like the PEG-NB-based hydrogels presented here, exhibit reproducibility and tunability of both biophysical properties and biochemical signaling molecules that can improve keratinocyte maintenance in culture.^[30] Maintaining keratinocyte stemness and extending proliferative lifespan in vitro will allow for long-term wound healing studies not possible with standard culture techniques. Ultimately, this finding enables researchers to better understand skin regeneration and translate these findings into tissue-engineered wound treatments.^[9–11,31]

5. Experimental Section

Macromer Synthesis: Norbornene-functionalized PEG was synthesized by combining PEG-hydroxyl (MW 10 kg mol⁻¹, 8-arm, hexaglycerol core; JenKemUSA) with a 5 \times molar ratio of pyridine and a 0.5 \times molar ratio of 4-(dimethylamino)pyridine (DMAP; Sigma-Aldrich) with respect to PEG hydroxyls in dichloromethane (DCM; Fisher Scientific). This PEG solution was then added to a mixture of 5-norbornene-2-carboxylic acid (10 \times molar ratio of with respect to PEG hydroxyls; Sigma-Aldrich) and *N,N'*-dicyclohexylcarbodiimide (DCC; Sigma-Aldrich) that was stirred for 30 minutes at room temperature under argon (Airgas). The subsequent reaction was stirred overnight under argon. The reaction solution was then filtered through filter paper in a Buchner funnel under vacuum and washed with 5% sodium bicarbonate (Sigma-Aldrich). PEG-norbornene (PEG-NB) solution was precipitated in ice-cold anhydrous diethyl ether (Fisher Scientific). The solution was then centrifuged at -10 °C and 4700 rpm for 10 min. The supernatant was decanted off and the remaining precipitate (PEG-NB product) was dried under vacuum overnight at room temperature. This product was then dialyzed in deionized water for at least two days at room temperature with water changes every 24 h. Dialyzed product was then flash frozen and lyophilized until dry. Proton nuclear magnetic resonance (¹H NMR, 500 MHz, deuterated chloroform) confirmed functionalization of PEG with norbornene by integration of peaks: δ 6.19–5.90 ppm (alkene protons from norbornene, m, 2H per arm), 4.26–4.12 ppm (ester

protons, m, 2H per arm), 3.73–3.54 ppm (ethylene glycol protons, m, 114H per arm).

Photoinitiator Synthesis: Equimolar amounts of dimethyl phenylphosphonite (Alfa Aesar) and 2,4,6-trimethylbenzoylphosphonite (Acros Organics) were added to a round-bottom flask and stirred for 18 h at room temperature under argon. In a separate beaker, a 4× molar ratio of lithium bromide with respect to dimethyl phenylphosphonite was dissolved in 100 mL of 2-butanone (Acros Organics). The reaction was stirred until all components dissolved and then this solution was added into the first reaction vessel. The subsequent reaction was heated to 50 °C and a precipitate formed after 10 min. The reaction solution was removed from heat and cooled to room temperature, filtered through filter paper in a Buchner funnel under vacuum, and rinsed with 2-butanone three times. Lithium phenyl (2,4,6-trimethylbenzoyl) phosphinate (LAP) product was dried under vacuum overnight at room temperature, dissolved in deionized water, frozen, and lyophilized until dry. ¹H NMR (500 MHz, deuterium oxide) was used to confirm LAP synthesis by integration of peaks: δ 7.55 ppm (m, 2H), 7.41 (m, 1H), 7.31 (m, 2H), 6.73 (s, 2H), 2.08 (s, 3H), and 1.86 (s, 6H).

Sample Fabrication: Thiol–ene hydrogels were polymerized using previously established methods.^[32,33] The hydrogel-forming precursor solution was created by combining 7.5 wt% 8-arm, 10 kg mol⁻¹ PEG-NB and DTT (Sigma-Aldrich), and 0.05 wt% LAP with various concentrations of cysteine-terminated peptides in sterile phosphate buffered saline (PBS, pH = 7.2; Life Technologies). Glass coverslips (18 mm; Fisher Scientific) were silanated with (3-mercaptopropyl)trimethoxysilane (Acros Organics) using a liquid-deposition technique.^[34] Hydrogels were photopolymerized in 90 μL drops placed between hydrophobic glass slides treated with SigmaCote (Sigma-Aldrich) and silanated 18 mm cover slips under 365 nm light at 10 mW cm⁻² for 5 min. Hydrogels were then swollen in PBS at for at least 18 h at 37 °C prior to use in experiments.

A design of experiments (DOE) approach interrogated the influence of integrin binding motif combinations and concentrations on HEKA stemness.^[35] This experimental method compared high and low concentrations of different binding motifs in peptides and proteins in the most statistically efficient way to analyze variable interdependence. Various combinations of three peptide sequences (Table 2) were covalently bound to PEG-NB hydrogel networks in concentrations similar to those quantified in human epidermal tissue.^[36–39] Reacting hydrogel precursors off stoichiometry with ratios ranging from 99.75:0.25 to 99.99:0.01 (norbornene to thiol) left free norbornene functional groups available to react with the cysteine residues on custom peptide chains.^[32] Custom peptides (GL Biochem, Boston) included CGRGDS to mimic fibronectin, CGYIGSR to emulate the binding portion of laminin, and CGGEFYDLRLKGDK (HepIII) to mimic a key adhesive component of the collagen IV triple helix.^[32,36,40] Corresponding standards, that is, protein-coated glass coverslips, were prepared using a protocol adapted from Li et al.^[41] Binding motif concentration was calculated by dividing the surface concentration of each protein by that protein's molecular weight and multiplying by the amount of binding motif present in each mole of protein.^[36,42–44] Fibronectin (Life Technologies), laminin (Life Technologies), and collagen IV (Sigma-Aldrich) were diluted in sterile PBS to concentrations listed in Table 2 and 0.5 mL drops were placed on clean 18-mm glass cover slips. After a 2-h incubation at room temperature under aseptic conditions, remaining material was aspirated and cover slips were stored at 4 °C until use.

Hydrogel Characterization: *E* of swollen hydrogel samples was measured as previously described.^[45] Briefly, hydrogel samples (height: 0.5 mm, diameter: 7 mm) were allowed to swell to equilibrium in PBS. The storage (*G'*) and loss moduli (*G''*) were measured for five replicates of each hydrogel formulation. Samples were subjected to shear at 1% strain through a dynamic angular frequency range of 0.1 to 100 rad s⁻¹. *E* was calculated from *G'* for all sample conditions using a Poisson's ratio of 0.5 corresponding to an incompressible material.^[46] Dynamic shear modulus measurements were also recorded for three replicate samples of the 7.5 wt% hydrogel formulation during polymerization. Hydrogel precursor solution was loaded between 8 mm parallel plates on a Discovery Hybrid Rheometer 2 (TA Instruments) with a fixed gap

of 600 μm. Shear modulus measurements started at a frequency of 1 rad s⁻¹ and 1% strain, within the linear viscoelastic regime for these hydrogels. After 40 s polymerization was initiated by exposure to 365-nm light and subsequent changes in *G'* and *G''* moduli were recorded.

HEKA Culture: Primary adult human epidermal keratinocytes (HEKAs) isolated from adult skin (C0055C, ThermoFisher) were cultured in complete serum-free growth media (EpiLife Medium, 30 μg mL⁻¹ bovine serum albumin, 5 μg mL⁻¹ bovine transferrin, 11 ng mL⁻¹ hydrocortisone, 10 ng mL⁻¹ rhGF-1, 18 ng mL⁻¹ PGE₂, and 1 ng mL⁻¹ rhEGF; EpiLife Defined Growth Supplement, ThermoFisher). HEKAs were seeded between passages four to six on samples in triplicate at 6000 cells cm⁻². Media was changed every 48 h until 50% confluency, then every 24 h thereafter.

Immunofluorescent Staining Protocol: Samples for stemness experiments were processed on day 7, day 14, and day 21, then fixed, stained for K₁ and K₁₄, and mounted for imaging, while samples for integrin expression experiments were processed on day 2, then fixed, stained for integrin β₁, and mounted for imaging. Samples for Ki-67 proliferation experiments were processed on day 2, day 7, and day 14, then fixed, stained for Ki-67, and mounted for imaging. Samples were rinsed with PBS and fixed with 4% paraformaldehyde (Electron Microscopy Sciences) for 15 min at room temperature. Cells were permeabilized by incubating with 0.5% Triton X-100 in PBS for 15 min at room temperature. Permeabilization solution was replaced with blocking solution made of 5% bovine serum albumin (BSA; Fisher Scientific) in PBS for 1 h at room temperature to prevent nonspecific antibody binding. Chicken anti-human K₁₄ and rabbit anti-human K₁ polyclonal primary antibodies (Biolegend) for stemness, rabbit anti-human ITGβ₁ primary antibody (Biolegend) for integrin expression, or rabbit anti-human Ki-67 polyclonal primary antibody (ThermoFisher Scientific) for Ki-67 expression were diluted 1:500 in immunofluorescent (IF) solution made from 3% BSA and 0.1% Tween 20 (ThermoFisher Scientific) in PBS and applied to samples for 1 h at room temperature. After rinsing with IF solution, samples were incubated with goat anti-chicken AlexaFluor 555 (for stemness) and goat anti-rabbit AlexaFluor 488 secondary antibodies (for stemness, integrin expression, and Ki-67 expression; all secondary antibodies from ThermoFisher) diluted 1:400 in IF solution for 1 h at room temperature. Secondary antibodies were replaced with DAPI (0.5 μg mL⁻¹ in PBS) for 10 min at room temperature. Sample cover slips with 18 mm diameter were mounted under 25 mm cover slips with Prolong Gold Antifade reagent (Life Technologies) for imaging.

Fluorescent Image Acquisition: Images were acquired on an Olympus BX63 fluorescent microscope. Three random fields of view were imaged at 10× magnification on each of three sample replicates. Corrected total cell fluorescence (CTCF) was calculated in ImageJ using the integrated density of the total image with background fluorescence subtracted:

$$\text{CTCF} = \text{Integrated density} - (\text{Area of image} \times \text{Mean fluorescence of background})$$

CTCF was normalized to fluorophore extinction coefficient after calculation.

Statistical Analysis: Outliers in the data were identified and removed using the ROUT Method (*Q* = 1%; GraphPad Prism 7 Software, San Diego, CA). Data are presented as mean ± SEM, *n* = 3 biological replicates, and *n* = 3 or 4 technical replicates for each experiment involving cell culture. JMP software (SAS, Cary, NC) generated the hydrogel conditions and analyzed the resulting data. The stemness results were entered back into the software and analyzed using a least-squares regression model to determine significance of the factors and plot the predicted responses. Data from technical replicates were pooled for analysis if a two-sided *F* test failed to reject the null hypothesis of equal variance with *p* > 0.05. One-way analysis of variance (ANOVA) tests were conducted to determine unequal means between platform data sets. Dunnett's or Tukey's multiple comparison tests were conducted post-hoc to find significant differences between sample and control means with a 95% confidence interval (GraphPad Prism 7 Software, San Diego, CA).

Supporting Information

Supporting Information is available from the Wiley Online Library or from the author.

Acknowledgements

This work was supported by funding from the Skin Disease Research Center Pilot and Feasibility Award, National Institute of Arthritis and Musculoskeletal and Skin Diseases Grant P30-AR-057212 (to C.M.M.) and the National Heart, Lung and Blood Institute Grant T32-HL-072738-14 (to D.D.-H.).

Conflict of Interest

The authors declare no conflict of interest.

Keywords

extracellular matrix, hydrogels, keratinocytes, peptides, poly(ethylene glycol)

Received: February 18, 2019

Revised: June 20, 2019

Published online: August 23, 2019

- [1] F. M. Watt, *Dev. Cell* **2016**, *38*, 601.
 [2] G. Donati, F. M. Watt, *Cell Stem Cell* **2015**, *16*, 465.
 [3] M. S. Tjin, A. W. C. Chua, D. R. Ma, S. T. Lee, E. Fong, *Macromol. Biosci.* **2014**, *14*, 1125.
 [4] C. M. DiPersio, R. Zheng, J. Kenney, L. Van De Water, *Cell Tissue Res.* **2016**, *365*, 467.
 [5] F. M. Watt, *EMBO J.* **2002**, *21*, 3919.
 [6] F. M. Watt, H. Fujiwara, *Cold Spring Harbor Perspectives in Biology*, Cold Spring Harbor Laboratory Press, Cold Spring Harbor, NY **2011**, pp. 3.
 [7] N. Ojeh, B. Akgul, M. Tomic-Canic, M. Philpott, H. Navsaria, *PLoS One* **2017**, *12*, e0174389.
 [8] J. Schweizer, in *Molecular Biology of the Skin* (Eds: M. Darmon, M. Blumenberg), Academic Press, Cambridge, MA **1993**, pp. 33.
 [9] L. Braiman-Wiksmann, I. Solomonik, R. Spira, T. Tennenbaum, *Toxicol. Pathol.* **2007**, *35*, 767.
 [10] G. D. Winter, *Adv. Exp. Med. Biol.* **1977**, *94*, 673.
 [11] M. Norouzi, S. M. Boroujeni, N. Omidvarkordshouli, M. Soleimani, *Adv. Healthcare Mater.* **2015**, *4*, 1114.
 [12] G. Bilousova, D. R. Roop, *Methods Mol. Biol.* **2013**, *961*, 337.
 [13] L. M. Wilkins, S. R. Watson, S. J. Prosky, S. F. Meunier, N. L. Parenteau, *Biotechnol. Bioeng.* **1994**, *43*, 747.
 [14] M. N. Nicholas, J. Yeung, *J. Cutaneous Med. Surg.* **2017**, *21*, 23.
 [15] W. S. Ramsey, W. Hertl, E. D. Nowlan, N. J. Binkowski, *In Vitro* **1984**, *20*, 802.
 [16] X. Liang, S. A. Boppart, *IEEE Trans. Biomed. Eng.* **2010**, *57*, 953.
 [17] A. J. Zhu, I. Haase, F. M. Watt, *Proc. Natl. Acad. Sci. U. S. A.* **1999**, *96*, 6728.
 [18] M. Gonzales, K. Haan, S. E. Baker, M. Fitchmun, I. Todorov, S. Weitzman, J. C. Jones, *Mol. Biol. Cell* **1999**, *10*, 259.
 [19] J. Salber, S. Gräter, M. Harwardt, M. Hofmann, D. Klee, J. Dujic, H. Jinghuan, J. Ding, S. Kippenberger, A. Bernd, J. Groll, J. P. Spatz, M. Möller, *Small* **2007**, *3*, 1023.
 [20] J. L. Ifkovits, J. A. Burdick, *Tissue Eng.* **2007**, *13*, 2369.
 [21] J. Zhu, R. E. Marchant, *Expert Rev. Med. Devices* **2011**, *8*, 607.
 [22] M. M. Movahednia, F. K. Kidwai, Y. Zou, H. J. Tong, X. Liu, I. Islam, W. S. Toh, M. Raghunath, T. Cao, *Tissue Eng., Part A* **2015**, *21*, 1432.
 [23] A. Pozzi, K. K. Wary, F. G. Giancotti, H. A. Gardner, *J. Cell Biol.* **1998**, *142*, 587.
 [24] J. C. Murray, G. Stingl, H. K. Kleinman, G. R. Martin, S. I. Katz, *J. Cell Biol.* **1979**, *80*, 197.
 [25] F. M. Watt, M. D. Kubler, N. A. Hotchin, L. J. Nicholson, J. C. Adams, *J. Cell Sci.* **1993**, *106*, 175.
 [26] A. L. Clement, T. J. Moutinho, Jr., G. D. Pins, *Acta Biomater.* **2013**, *9*, 9474.
 [27] F. M. Watt, *EMBO J.* **2002**, *21*, 3919.
 [28] J. C. Adams, F. M. Watt, *Nature* **1989**, *340*, 307.
 [29] F. M. Watt, H. Green, *Nature* **1982**, *295*, 434.
 [30] L. E. Dickinson, S. Gerecht, *Front. Physiol.* **2016**, *7*, 341.
 [31] G. D. Mogosanu, A. M. Grumezescu, *Int. J. Pharm.* **2014**, *463*, 127.
 [32] S. T. Gould, N. J. Darling, K. S. Anseth, *Acta Biomater.* **2012**, *8*, 3201.
 [33] M. Tsunenaga, E. Adachi, S. Amano, R. E. Burgeson, T. Nishiyama, *Matrix Biol.* **1998**, *17*, 603.
 [34] B. Arkles, *Silane Coupling Agents: Connecting Across Boundaries*, Gelest Inc., Morrisville, PA **2014**.
 [35] G. E. Box, W. G. Hunter, J. S. Hunter, *Statistics for Experimenters: Design, Innovation, and Discovery*, Wiley, New York **2005**.
 [36] M. S. Wilke, L. T. Furcht, *J. Invest. Dermatol.* **1990**, *95*, 264.
 [37] J. P. Kim, K. Zhang, J. D. Chen, K. C. Wynn, R. H. Kramer, D. T. Woodley, *J. Cell. Physiol.* **1992**, *151*, 443.
 [38] M. Kubo, M. Kan, M. Isemura, I. Yamane, H. Tagami, *J. Invest. Dermatol.* **1987**, *88*, 594.
 [39] A. Takashima, F. Grinnell, *J. Invest. Dermatol.* **1985**, *85*, 304.
 [40] M. H. Fittkau, P. Zilla, D. Bezuidenhout, M. P. Lutolf, P. Human, J. A. Hubbell, N. Davies, *Biomaterials* **2005**, *26*, 167.
 [41] X. Li, A. Contreras-Garcia, K. LoVetri, N. Yakandawala, M. R. Wertheimer, G. De Crescenzo, C. D. Hoemann, *J. Biomed. Mater. Res., Part A* **2015**, *103*, 3736.
 [42] H. Sage, R. G. Woodbury, P. Bornstein, *J. Biol. Chem.* **1979**, *254*, 9893.
 [43] M. Sasaki, H. K. Kleinman, H. Huber, R. Deutzmann, Y. Yamada, *J. Biol. Chem.* **1988**, *263*, 16536.
 [44] R. Timpl, H. Rohde, P. G. Robey, S. I. Rennard, J. M. Foidart, G. R. Martin, *J. Biol. Chem.* **1979**, *254*, 9933.
 [45] C. M. Kirschner, D. L. Alge, S. T. Gould, K. S. Anseth, *Adv. Healthcare Mater.* **2014**, *3*, 649.
 [46] S. Joas, G. E. M. Tovar, O. Celik, C. Bonten, A. Southan, *Gels* **2018**, *4*, 69.
 [47] S. E. Ochsenhirt, E. Kokkoli, J. B. McCarthy, M. Tirrell, *Biomaterials* **2006**, *27*, 3863.
 [48] Y. Feng, M. Mrksich, *Biochemistry* **2004**, *43*, 15811.
 [49] A. J. García, J. E. Schwarzbauer, D. Boettiger, *Biochemistry* **2002**, *41*, 9063.
 [50] J. D. Humphries, A. Byron, M. J. Humphries, *J. Cell Sci.* **2006**, *119*, 3901.
 [51] J. D. Parkin, J. D. San Antonio, V. Pedchenko, B. Hudson, S. T. Jensen, J. Savige, *Hum. Mutat.* **2011**, *32*, 127.
 [52] J. Khoshnoodi, V. Pedchenko, B. G. Hudson, *Microsc. Res. Tech.* **2008**, *71*, 357.